

# Reliable Assessment of Rainfall-Induced Slope Instability

## 강우로 인한 사면의 불안정성에 대한 신뢰성 있는 평가

Kim, Yun-Ki<sup>1</sup> 김 윤 기 Choi, Jung-Chan<sup>1</sup> 최 정 찬  
Lee, Seung-Rae<sup>2</sup> 이 승 래 Seong, Joo-Hyun<sup>3</sup> 성 주 현

### 요 지

강우침투로 인하여 많은 사면이 붕괴되고 있다. 따라서 사면에 대한 최근 연구들은 강우가 유발하는 사면의 불안정성에 초점이 맞춰져 있으며 강우침투 문제는 중요한 사면붕괴 발생 요인으로 인식되고 있다. 강우가 사면 내부의 모관흡수력을 감소시키면서 사면 내부로 침투되며 심지어 지반특성에 따라 표층 부근에서 양의 간극수압이 발생할 수도 있다. 이러한 현상은 사면의 강도를 감소시켜 사면 붕괴를 유발할 수 있다. 국내 여러 공공기관에서는 지하수위가 표층 또는 일정 깊이 내에 존재하도록 하여 사면의 포화상태를 가정하는 보수적인 사면 설계방안을 제시하였으나, 이러한 가정은 대부분 부적절하고 이를 만족시키기 위해 때로는 사면설계 단계에서 잘못된 지반물성이 사용되기도 한다. 본 논문에서는 실제 강우침투 현상을 고려하여 보다 합리적으로 사면의 안정성을 평가하는 기법이 제안되었다. 국내 풍화토에 대한 불포화 지반물성(강도, 함수특성곡선, 투수곡선)이 실험적으로 획득되었으며, 인공신경망 모델을 통해 간접적으로도 추정되었다. 또한 현장 계측자료의 불확실성을 보완하기 위하여 사면의 불안정성 평가기법에 대하여 결정론적 해석과 확률론적 해석에 기반한 실시간 사면 붕괴 경보 기준이 모니터링 시스템에 도입되었다. 이러한 사면안정성 평가기법은 사면 내부의 모관흡수력, 함수비와 같은 중요요소를 계측한 현장자료와 접목하여 강우에 따라 불안정해진 사면에 대한 조기 경보시스템으로 활용될 수 있다.

### Abstract

Many slope failures are induced by rainfall infiltration. A lot of recent researches are therefore focused on rainfall-induced slope instability and the rainfall infiltration is recognized as the important triggering factor. The rainfall infiltrates into the soil slope and makes the matric suction lost in the slope and even the positive pore water pressure develops near the surface of the slope. They decrease the resisting shear strength. In Korea, a few public institutions suggested conservative slope design guidelines that assume a fully saturated soil condition. However, this assumption is irrelevant and sometimes soil properties are misused in the slope design method to fulfill the requirement. In this study, a more relevant slope stability evaluation method is suggested to take into account the real rainfall infiltration phenomenon. Unsaturated soil properties such as shear strength, soil-water characteristic curve and permeability for Korean weathered soils were obtained by laboratory tests and also estimated by artificial neural network models. For real-time assessment of slope instability, failure warning criteria of slope based on deterministic and probabilistic analyses were introduced to complement uncertainties of field measurement data. The slope stability evaluation technique can be combined with field measurement data of important factors, such as matric suction and water content, to develop an early warning system for probably unstable slopes due to the rainfall.

**Keywords :** Probabilistic analysis, Rainfall infiltration, Slope design, Slope stability, Unsaturated soil

1 정회원, KAIST 건설및환경공학과 박사과정 (Member, Graduate Student, Dept. of Civil & Envir. Engrg., KAIST)

2 정회원, KAIST 건설및환경공학과 교수 (Member, Prof., Dept. of Civil & Envir. Engrg., KAIST, srlee@kaist.ac.kr, 교신저자)

3 정회원, 한국시설안전관리공단 기술개발팀 대리 (Member, Assistant Manager, R&D Division, KISTEC)

\* 본 논문에 대한 토의를 원하는 회원은 2009년 11월 30일까지 그 내용을 학회로 보내주시기 바랍니다. 저자의 검토 내용과 함께 논문집에 게재하여 드립니다.

## 1. Introduction

Many slope failures have occurred in Asian region during rainy season. Especially, the intensive rain storms and typhoons induced sudden slope failures and these disasters brought great economic losses and casualties.

A few Korean public institutions suggested conservative slope design guidelines that assume a fully saturated soil condition. In spite of this conservative assumption, many slopes continue to fail, as this assumption is irrelevant to real natural phenomenon and sometimes soil properties are misused in the slope design method. Therefore, more relevant slope stability evaluation method is necessary to take into account the real rainfall infiltration phenomenon.

Combined seepage and stability analyses of slopes can be performed using unsaturated soil mechanics concept. Unsaturated soil properties such as shear strength, soil-water characteristic curve and permeability of unsaturated soils are used for accurate prediction. However, the laboratory tests to obtain these soil properties are troublesome and time-consuming. This difficulty of laboratory tests has prevented the practical use of unsaturated slope stability evaluation method considering the rainfall infiltration.

In this study, the mechanism of slope failures triggered by rainfall infiltration was mentioned and the problem of current slope design guideline was discussed. Besides, to obtain the unsaturated soil properties, an indirect and simple estimation method by artificial neural network was suggested. Measurements of matric suction and water content in a slope were also conducted to monitor the unsaturated characteristics during the rainfall in real-time. From these results, failure warning criteria of slope based on deterministic and probabilistic analyses were suggested.

## 2. Rainfall-Induced Slope Instability

The mechanism of rainfall induced slope failures is the most fundamental aspect to be considered in the slope stability evaluation. If ground water table is near the surface and the conductivity of soil is high due to cracks and joints, the slope can be easily saturated during rainfall

events. In this condition, circular and deep slope failures are usually induced. This viewpoint is similar to the rationalization which says that the matric suction in slopes can be ignored when considering the long-term stability of slopes (Fredlund, 1995).

However, most of soil slopes exist in an unsaturated soil condition with a deep ground water table. Negative pore-water pressures develop in the unsaturated condition, and they keep the slope in a more stable state. This negative pore water pressure is also called matric suction. It is difficult to fully saturate the slopes in the case of a deep ground water table condition. The infiltrated rainfall cannot reach the deep depth because the conductivity of the soil in an unsaturated condition is generally very low and the soil has high water storage capacity to store the water in soil pores.

Rainfall infiltrates the slope from the surface and decreases the matric suction as shown in Fig. 1. The wetting depth is affected by many factors such as rainfall condition, soil conductivity, and soil stratification. In that case, the strength of soil decreases as the matric suction decreases or disappears. Positive pore water pressure can also develop due to a temporary water table near the slope surface, decreasing the soil strength suddenly. Slope failures occur if the infiltrated rainfall reaches to a critical depth. Most of these failures are shallow or surface types. Therefore, in this type of slope failure, the matric suction and water content inside the slopes have been recognized as the most important soil properties directly related to the instability of the slope.

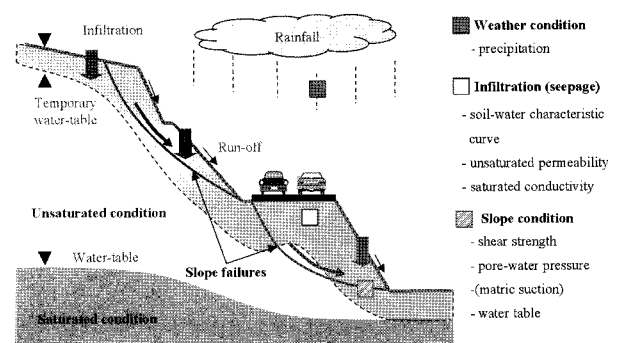


Fig. 1. Mechanism of rainfall-induced slope failure

### 3. Problems in Current Slope Design Guideline

#### 3.1 Assumption of Water Table

To consider the effect of rainfall infiltration, current slope design guidelines recommend that the water-table be located at slope surface or at a certain depth near the surface in case of rainy condition. That is, it assumes that the slope is fully saturated up to the surface as shown in Fig. 2. To satisfy this condition, the rainfall must infiltrate the soil easily through cracks with high conductivity in the condition of initially high water-table and thus the water-table rises to the surface. However, it is very hard to satisfy this condition in mountains and man-made slopes. Moreover, the rainfall should continue for very long time since the slopes composed of weathered residual soils in Korea have low permeability values. The hydrostatic water pressure in the fully saturated condition also cannot be developed due to the water flow according to the hydraulic gradient. Therefore, it is irrelevant to evaluate the slope stability assuming that the slope is fully saturated.

#### 3.2 Improper Soil Properties

In current slope design guidelines, the minimum factor of safety calculated from limit equilibrium method must be higher than suggested values; 1.5 for dry season and 1.2~1.3 for wet season. This guideline is judged to be quite conservative as the slope has sufficient extra stability. However, for reliable slope stability evaluation, input soil properties such as shear strength must be obtained properly.

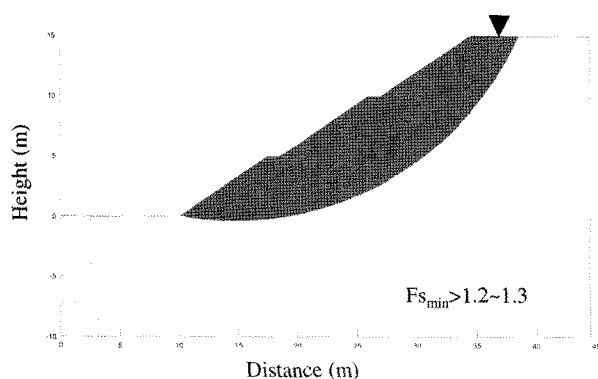


Fig. 2. Irrelevant assumption of water table at surface in current slope design guideline

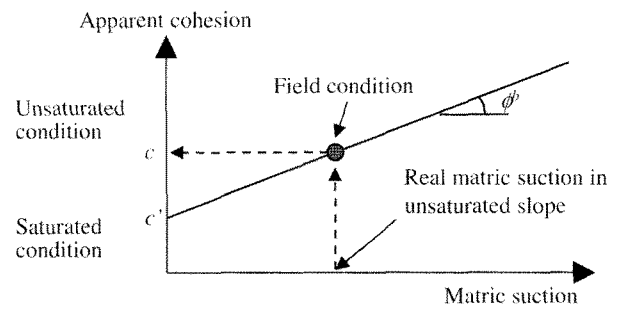


Fig. 3. Misread soil properties for slope design

The shear strength of soil obtained from site investigation is applied to both slope stability analyses for dry season and wet season. That is, the difference between dry condition and wet condition is only the level of water table. It is required to check how the shear strength was obtained. It is general to obtain the soil properties such as cohesion and frictional angle from direct shear tests using undisturbed unsaturated soil samples. These values are directly applied for the stability analysis. However, the shear strength in a saturated condition is reduced with the loss of matric suction as the obtained cohesion ( $c$ ) includes the effective cohesion ( $c'$ ) and the increased strength related to the matric suction as shown in Fig. 3. This reduced cohesion has a negative role in the slope stability.

As a result, this misread soil properties might be one of the reasons for frequent slope failures during wet season, in spite of designing the slope by applying the very conservative water table condition. However, it is not so simple to use the saturated shear strength for wet season. If the saturated shear strength is used for slopes, it is difficult to maintain the suggested factor of safety of slopes. To keep the slopes stable, more gentle or reinforced slopes are required. In such slopes, efficient and economical construction is impossible as the cost increases. Therefore, it is necessary to develop an optimized slope design guideline considering the local rainfall condition and the local soil characteristics rather than the slope design method to use the shear strength with the standardized slope.

### 4. Slope Stability Evaluation to Consider Rainfall Infiltration

Distribution of matric suction in a slope can be predicted

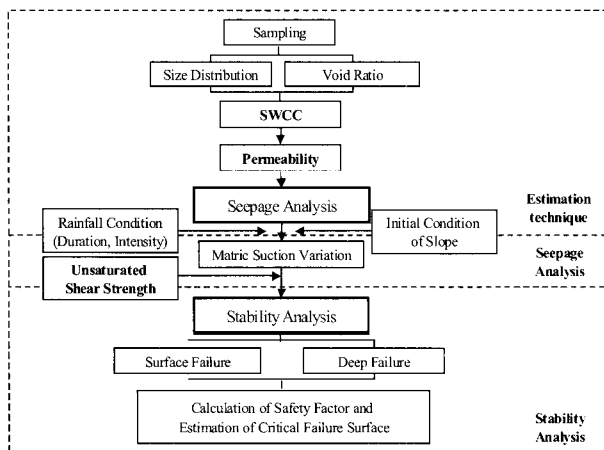


Fig. 4. Flowchart of slope stability evaluation to consider rainfall infiltration

by a numerical seepage analysis with unsaturated soil properties such as soil-water characteristic curve and unsaturated permeability function. The initial matric suction and rainfall condition must be assumed to consider the field condition because they have large effects on the seepage behavior in a slope. By conducting the slope stability analysis with the distribution of matric suction obtained from the seepage analysis, the factor of safety of slope is calculated and the failure surface can be predicted. This slope stability evaluation method also considers the mechanism of real slope failure during rainfall. The slope stability evaluation technique suggested to consider the rainfall infiltration is depicted in Fig. 4. This guideline is composed of three parts: Estimation of soil properties, seepage analysis, and slope stability evaluation. To consider the effect of rainfall infiltration in slopes, the unsaturated soil properties are used as input in seepage analysis. By introducing the simple estimation techniques of unsaturated soil properties, difficult and time-consuming laboratory tests can be skipped in practical use.

The results obtained from the numerical analysis can be utilized as a basis to judge slope instability as shown in Fig. 5. Slope failure warning system was developed to prevent sudden slope failures due to rainfall infiltration and to provide suitable reinforcement of slopes. The infiltration depth is estimated by real-time monitoring of important factors. Comparing the infiltration depth with the result of numerical prediction, the degree of danger for slope failures can be determined and alarmed. In

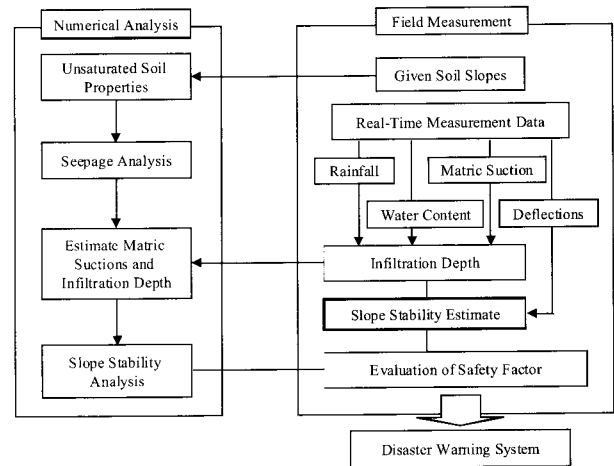


Fig. 5. Slope failure warning system according to rainfall infiltration

practice, this system can be applied for more economical construction, maintenance and reinforcement of slopes.

## 5. Unsaturated Soil Properties

Important unsaturated soil properties are composed of shear strength, soil-water characteristic curve and unsaturated permeability function to simulate the behavior of unsaturated slope. Soil-water characteristic curve represents a relationship between the matric suction and water content in soil. The lower the water content is, the higher the matric suction is. This amount of water content has a close relationship not only with soil permeability but also with shear strength of soil. As the water content decreases in soil, the soil permeability decreases and shear strength increases with higher matric suction. According to these characteristics of unsaturated soil, the unsaturated soil properties are usually used to analyze water flow and soil behavior in unsaturated condition.

These unsaturated soil properties of Korean soils have not been obtained sufficiently as laboratory tests are difficult and time-consuming to conduct. Therefore, indirect estimation methods have been suggested using simple soil properties such as particle size distribution (Burdine, 1953; Mualem, 1976; Arya & Paris, 1981; Rawls & Brakensiek, 1985).

### 5.1 Unsaturated Shear Strength

Fredlund et al. (1978) suggested the following equation

for representing unsaturated shear strength.

$$\tau_f = c' + (\sigma_n - u_a) \tan \phi' + (u_a - u_w) \tan \phi^b \quad (1)$$

where,  $\tau_f$  = shear strength;  $c'$  = effective cohesion;  $(\sigma_n - u_a)$  = net normal stress;  $\phi'$  = friction angle;  $(u_a - u_w)$  = matric suction; and  $\phi^b$  = soil property related to the matric suction.

In the range of very low matric suction,  $\phi^b$  is equal to  $\phi'$  as the soil maintains saturated condition. However, the soil becomes unsaturated as the matric suction increases higher than the air-entry value. As a result, the amount of increased shear strength due to the increase of matric suction is lower than that due to the increase of net confining normal stress. The nonlinearity of  $\phi^b$  between shear strength and the matric suction is proven by experimental results and increases in a wide range of matric suction (Gan et al., 1986; Fredlund et al., 1978; Escario & Juca, 1989).

Lee et al. (2003) suggested a hyperbolic equation to consider the nonlinearity and represented the behavior of apparent cohesion as a simple formulation (Fig. 6). The hyperbolic equation can be formulated by an initial slope and an ultimate value related to the friction angle ( $\phi'$ ) and the ultimate increment of apparent cohesion ( $C_{max}$ ), respectively.  $C_{max}$  indicates maximum amount of increasing

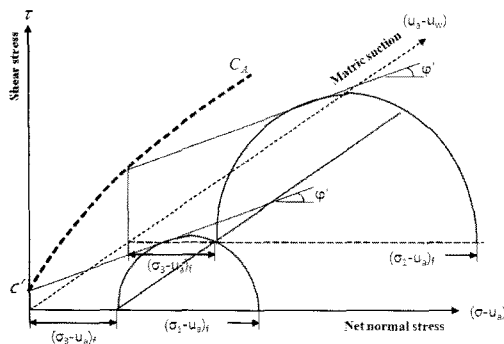


Fig. 6. Nonlinear unsaturated shear strength

apparent cohesion induced only by matric suction.

$$C_A = c' + \frac{(u_a - u_w)}{1 / \tan \phi' + (u_a - u_w) / C_{max}} \quad (2)$$

The estimation method for  $C_{max}$  was developed using artificial neural network models based on experimental results of Korean weathered granite soils (Fig. 7). In this paper, a simple equation is suggested with coefficients calculated from weights and bias of artificial neural network in Eq. (3). In Eqs. (4) and (5),  $P_1$  and  $P_2$  mean sand contents and clay&silt contents, and  $P_3$ ,  $P_4$ ,  $P_5$ , and  $P_6$  are void ratio, compacted water content, effective cohesion, and friction angle, respectively. The parameters are summarized in Table 1.

$$Target(C_{max}) = t_0 + t_1 / (1 + \exp(A)) + t_2 / (1 + \exp(B)) \quad (3)$$

$$A = ta_0 + ta_1 \times P_1 + ta_2 \times P_2 + ta_3 \times P_3 + ta_4 \times P_4 + ta_5 \times P_5 + ta_6 \times P_6 \quad (4)$$

$$B = tb_0 + tb_1 \times P_1 + tb_2 \times P_2 + tb_3 \times P_3 + tb_4 \times P_4 + tb_5 \times P_5 + tb_6 \times P_6 \quad (5)$$

## 5.2 Soil-water Characteristic Curve

Soil-water characteristic curve (SWCC) is the basic soil property to determine the characteristics of unsaturated soil. Fig. 8 plots a typical shape of SWCC.

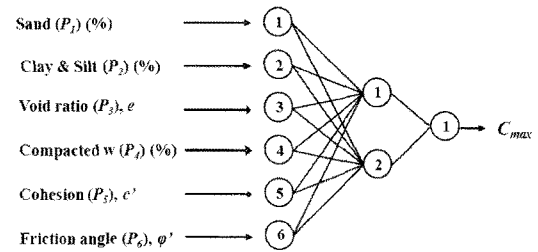


Fig. 7. ANN structure to estimate shear strength (Lee et al., 2003)

Table 1. Parameters to determine nonlinear shear strength

Target	$t_0$	$t_1$	$t_2$	$ta_0$	$ta_1$	$ta_2$	$ta_3$	$ta_4$	$ta_5$	$ta_6$
				$tb_0$	$tb_1$	$tb_2$	$tb_3$	$tb_4$	$tb_5$	$tb_6$
$C_{max}$	238.352	98.588	-228.984	-0.2299	0.005	-0.0079	0.0018	-0.0273	-0.024	0.0171
				0.2926	-0.0126	0.019	-1.7254	0.0922	0.1074	-0.0186

The estimation method for fitting parameters of Fredlund & Xing's SWCC (Eq. (6)) was suggested also using the artificial neural network presented in Fig. 9 (Lee, 2004). Four parameters ( $a$ ,  $n$ ,  $m$ ,  $s$ ) are required to define the SWCC. However,  $m$  parameter related to the residual water content can be assumed to be a constant value of 1.7 according to the experimental results. The saturated water content obtained from the experiments is used as  $s$  parameter to consider the change of void ratio during the tests.

The difference of experimental and theoretical saturated water content ( $\Delta s = s - \theta_{theoretical}$ ) is used in the estimation technique to define  $s$ .

$$\theta = \frac{s}{\left[ \ln \left[ e + \left( \frac{u_a - u_w}{a} \right)^n \right] \right]^m} \quad (6)$$

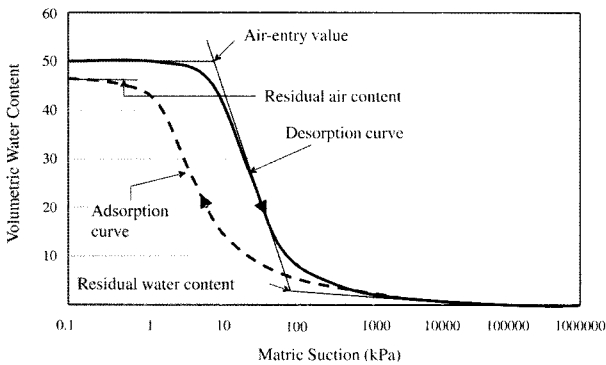


Fig. 8. Soil-water characteristic curve

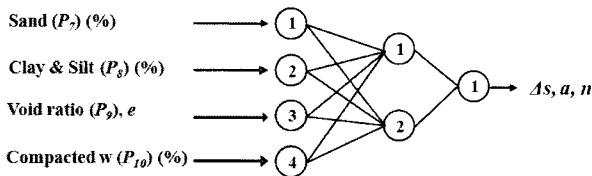


Fig. 9. ANN structure to estimate SWCC (Lee, 2004)

where,  $\theta$  = volumetric water content;  $s$  = saturated water content, and  $a$ ,  $n$ ,  $m$  = fitting parameters.

A simple equation is represented by Eq. (7) and parameters are summarized in Table 2.

$$Target(\Delta s, a, n) = t_0 + t_1 / (1 + \exp(C)) + t_2 / (1 + \exp(D)) \quad (7)$$

$$C = tc_0 + tc_1 \times P_7 + tc_2 \times P_8 + tc_3 \times P_9 + tc_4 \times P_{10} \quad (8)$$

$$D = td_0 + td_1 \times P_7 + td_2 \times P_8 + td_3 \times P_9 + td_4 \times P_{10} \quad (9)$$

### 5.3 Unsaturated Permeability Function

The permeability of unsaturated soils is not constant and can be represented as a function of matric suction or water content (degree of saturation). Fig. 10 illustrates the characteristics of reduced permeability as the matric suction increases. The permeability of sandy soil has higher permeability in the range of low matric suction but clayey soil has higher value in high matric suction. The permeability function has a close relationship with SWCC because the function is changed according to the amount of water content in soil, which is represented by SWCC. Therefore, the permeability function and SWCC exhibit similar shapes.

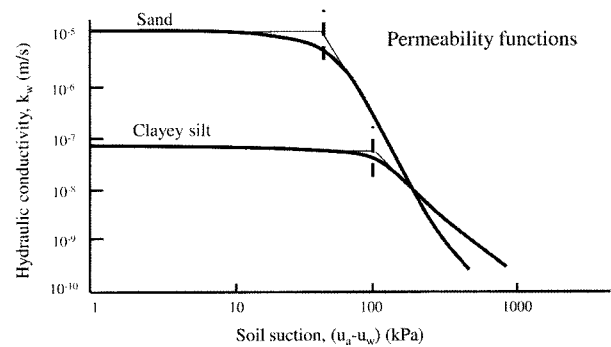


Fig. 10. Unsaturated permeable function

Table 2. Parameters to determine SWCC

Target	$t_0$	$t_1$	$t_2$	$tc_0$	$tc_1$	$tc_2$	$tc_3$	$tc_4$
				$td_0$	$td_1$	$td_2$	$td_3$	$td_4$
$\Delta s$	0.0386	0.1343	-0.1476	1.7709	-0.0402	-0.047	3.2665	-0.0205
				-0.3891	0.0208	0.033	-4.4745	-0.143
$a$	84.0193	101.2989	-111.953	-0.3096	-0.0064	-0.047	3.1025	0.0068
				0.3197	0.008	0.0506	-3.454	-0.0012
$n$	0.8857	0.577	-0.6099	1.9223	-0.0202	-0.0466	0.8755	0.0149
				-2.0076	0.0211	0.0483	-0.8885	-0.0156

Fredlund et al. (1994) suggested Eq. (10) to estimate the unsaturated permeability function from SWCC.

$$k_r(\psi) = \frac{\int_{\psi}^{\psi_r} \frac{\theta(\vartheta) - \theta(\psi)}{\vartheta^2} \theta'(\vartheta) d\vartheta}{\int_{\psi_{aev}}^{\psi_r} \frac{\theta(\vartheta) - \theta(\psi)}{\vartheta^2} \theta'(\vartheta) d\vartheta} \quad (10)$$

where  $k_r$  = relative coefficient of permeability;  $\psi$  is the matric suction ( $u_a - u_w$ );  $\psi_r$  = residual matric suction;  $\psi_{aev}$  = air entry value; and  $\vartheta$  = dummy variable.

Kim (2003) and Cui (2007) modified this equation using a fitting additional parameter ( $\Theta^q$ ) to estimate more accurate function based on the experimental results.

#### 5.4 Infinite Slope Stability Evaluation of Shallow Slope Failure

Factor of safety (FS) of an infinite slope can be used as the slope stability evaluation of shallow slope failure which is parallel to the slope surface (Rahardjo et al., 1994; Fourie et al., 1999; Cho and Lee, 2002).

Unsaturated soil slope considering the matric suction and stress state can be written as follows.

$$FS = \frac{c' + \{\gamma z_w \cos^2 \alpha + (u_a - u_w)\} \tan \phi'}{\gamma z_w \sin \alpha \cos \alpha} \quad (11)$$

where, FS = factor of safety;  $c'$  = cohesion;  $\gamma$  = unit weight;  $(u_a - u_w)$  = matric suction;  $\phi'$  = friction angle,  $\phi^b$  = an angle defining the increase in shear strength by an increase in matric suction;  $z_w$  = vertical depth of slope; and  $\alpha$  = slope angle.

With nonlinear shear strength of unsaturated soil represented by Eq. (2), FS of shallow slip surface can be calculated by the following equation.

$$FS = \frac{c' + W \cos^2 a \tan \phi' + \frac{(u_a - u_w)}{1 / \tan \phi' + (u_a - u_w) / C_{max}}}{W \sin a \cos a} \quad (12)$$

where,  $W$  = weight of body considering the degree of saturation of soil; and  $\alpha$  = slope angle.

## 6. Field Measurements

Distributions of matric suction and water content in slopes are important factors in the problem of rainfall-induced slope instability. Variation of these factors must be continuously measured in slopes exposed to natural environments. If the range of variation can be defined, the result will be used in slope stability evaluation and this design method can be applied to practical affairs. The disaster warning system can also be developed from the real-time monitoring of the matric suction and water content directly measured in the field.

In this study, instruments such as tensiometers, WCRs (Water Content Reflectometers) and rain gauge were installed in a compacted roadside slope shown in Fig. 11. WCRs can detect the volumetric water content in a few seconds at each depth of slope and tensiometers measure the matric suction directly. These instruments were inserted into each 15 cm depth interval from surface to 60 cm depth. Measurement results are shown in Fig. 12. During measurements, highest and lowest matric suctions are 73 kPa and 3 kPa, respectively. The high matric suction was induced during no rainy days. After the rainfall, the matric suction showed the low value around 3 kPa.

The basic soil properties of this slope are shown in Table 3. The soil is clayey sand according to Unified Soil Classification System (USCS) (ASTM D 2487-93). The effective cohesion and friction angle is 10 kPa and 30° obtained by consolidated drained triaxial compression test. And the saturated permeability of soil is  $8 \times 10^{-6}$  m/s by ASTM D5084-03 Method C.

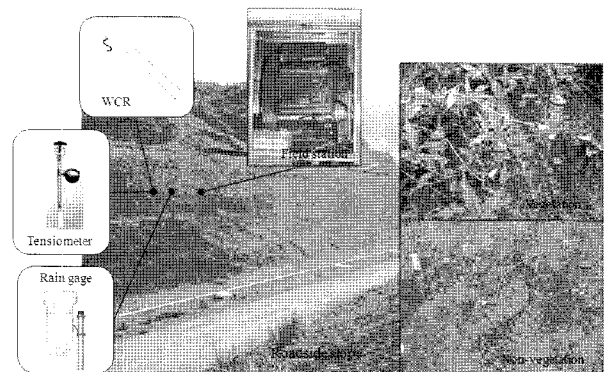
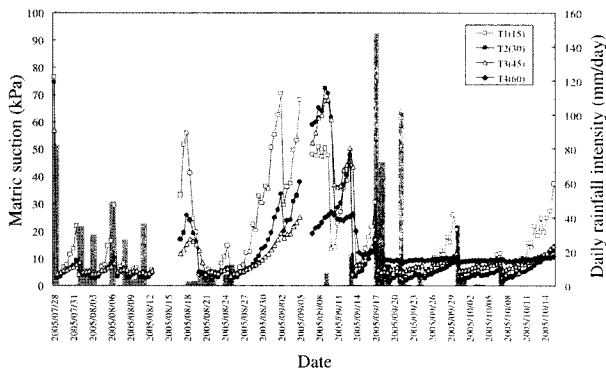
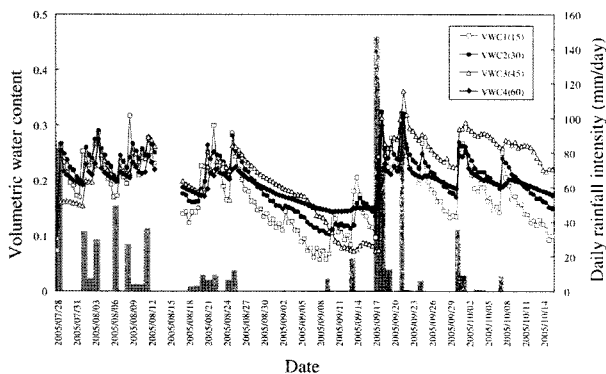


Fig. 11. Field measurements in slope

Wetting and drying processes at 15 cm and 30 cm depths around 17 September were plotted in Fig. 13. These gathered data represent the field soil-water characteristic curve (field SWCC). To simulate the infiltration of rainfall and the unsaturated flow of water in slope, seepage analysis was conducted with commercial finite element software SEEP/W (Geo-slope). The field SWCC was used as the input soil property in this analysis. Unsaturated permeability function was estimated from field SWCC by indirect estimation method (Fredlund et al. 1994). The



(a) Variation of matric suction



(b) Variation of water content

Fig. 12. Measurement results during rainy season

boundary condition of water flux was the pattern of unsteady natural rainfall intensity of rainfall event. To compare the results with measurements for each time, transient analyses were conducted. Results of numerical analyses were compared with that of field infiltration, as shown in Fig. 14. Solid lines in Fig. 14 mean transient

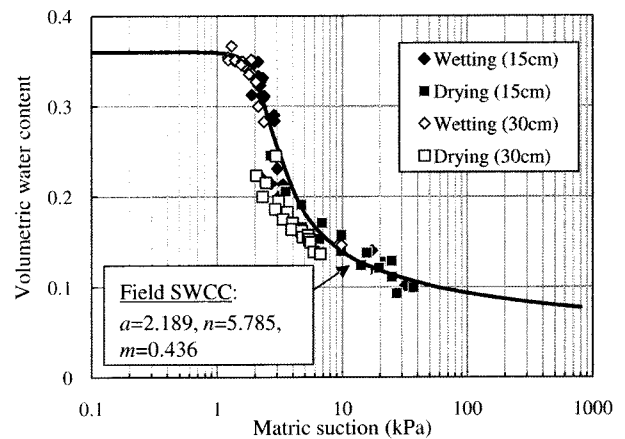


Fig. 13. Field soil-water characteristic curve from measurements in slope

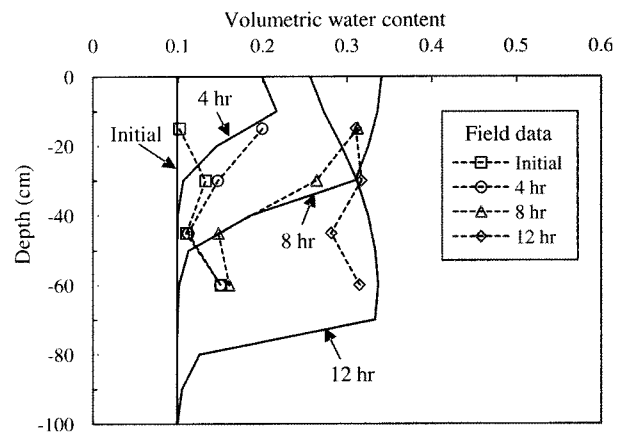


Fig. 14. Comparison of numerical analysis results using field SWCC (solid lines) with measured data in field (dashed lines)

Table 3. Basic soil properties of slope

Property	Value	Method
Gravel content	24.8%	ASTM D2487-93
Sand content	47.6%	
Clay & Silt content	27.6%	
USCS	SC	Sampling
Void ratio ( $e$ )	0.57	
Unit weight ( $\gamma$ )	17.56 kN/m <sup>3</sup>	Consolidated Drained triaxial compression test
Effective cohesion ( $c'$ )	10 kPa	
Friction angle ( $\phi'$ )	30°	
Saturated permeability ( $k_s$ )	8×10 <sup>-6</sup> m/s	ASTM D5084-03 Method C



distributions of water content predicted by numerical analysis with the field SWCC. Comparing the result with the measured data in field, the analysis using field SWCC showed a good agreement with the field data. Therefore it can be judged that the measurements in field slope are relatively reliable for monitoring slopes.

## 7. Slope Stability Evaluation

Using soil properties shown in Table 3, unsaturated soil properties of apparent cohesion and SWCC were estimated by Eqs. (3) and (7) to simulate the infiltration behavior of the slope. The parameters of unsaturated soil are shown in Table 4.

Selected rainfall conditions presented in Table 5 were applied for numerical analyses of seepage and slope stability to evaluate the long-term stability. Duration and intensity of each rainfall case are 23.8 mm/hr for 12 hours, 16.8 mm/hr for 24 hours and 13.6 mm/hr for 36

hours, respectively. These rainfall conditions were predicted by probabilistic rainfall characteristics of monitored region.

### 7.1 Deterministic Analysis

Deep and shallow slope failures were evaluated by seepage and slope stability analyses. Fig. 15 shows the pore-water pressure distributions according to the three rainfall cases (SEEP/W). As a result, there appeared positive pore-water pressure (perched water-table) near the surface. Wetting depths according to case 1, 2 and 3 were 0.6 m, 1.4 m and 2.3 m, respectively. In this slope, the duration of rainfall has more influence on the wetting depth than the rainfall intensity. Near the wetting front, the pore-water pressure decreased suddenly to initial value (20 kPa).

Wetting depth and deep slope shapes which have the minimum FS ( $FS_{min}$ ) are shown in Fig. 16. As the wetting depth increases,  $FS_{min}$  decreases a little. The shape of deep slope changed to the small circular type in case 3. However, the slope has enough stability for all rainfall cases.

Variations of FS at each slip surface depth are shown in Fig. 17. Results of seepage analysis (Fig. 15) were used as pore-water pressures and FS of shallow slope was calculated by Eq. (12). FS decreased with depth in wetted area. Near wetting front, FS increased suddenly as the soil existed in initial unsaturated condition. In rainfall case 3, FS at wetting front (1.31) approached to critical value 1.0, which was lower than that of 3 m depth (1.6). This means that shallow soil failure could occur.

The values of pore-water pressure according to 1.5, 1.2 and 1.0 values of FS were calculated for each depth and shown in Fig. 18. The stage of danger of slope failure could be separated into three parts. The slip has enough stability at  $FS > 1.5$ . In case of  $FS < 1.2$ , there is the

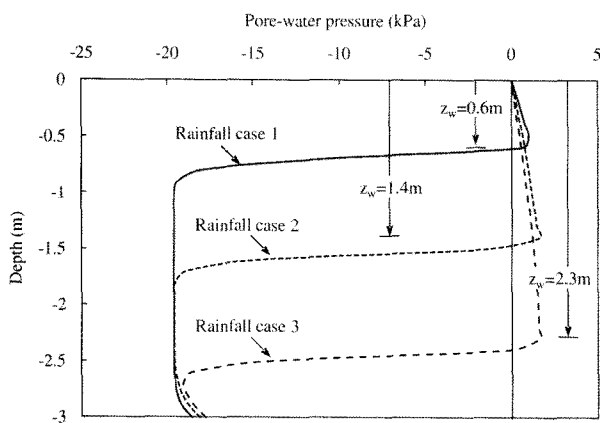


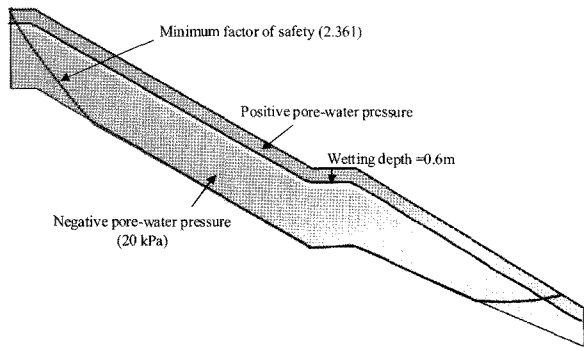
Fig. 15. Pore-water pressure distributions according to rainfall cases

Table 4. Estimated unsaturated soil properties

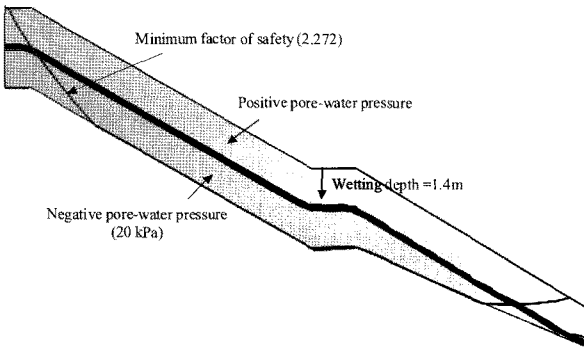
Parameters	SWCC			Shear strength
	$\Delta s$	$a$	$n$	$C_{max}$
Value	-0.02586	33.653	0.656	284.4

Table 5. Applied rainfall conditions

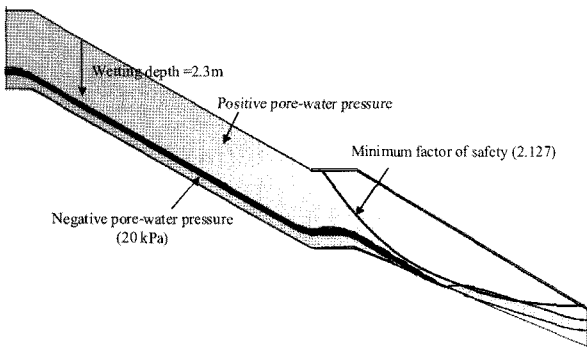
Rainfall	Rainfall intensity (mm/hr)	Rainfall duration (hour)	Total rainfall amount (mm)	Wetting depth from SEEP/W (m)	Minimum factor of safety from SLOPE/W
Case 1	23.8	12	286	0.6	2.361
Case 2	16.8	24	403	1.4	2.272
Case 3	13.6	36	490	2.3	2.127



(a) Rainfall case 1



(b) Rainfall case 2



(c) Rainfall case 3

Fig. 16. Wetting depths and deep slope shapes predicted by numerical analyses

possibility that the slip failure across the corresponding depth occurs. Each value of FS was assumed from the conventional slope design chart that had been used for a long time. If water infiltrates the slope and the slope near the surface is fully saturated, the hydrostatic condition could be developed. There will be no shallow slope failure less than 1.5 m in this slope condition as shown in Fig. 18. In the condition of the pore-water pressure for rainfall case 3, slip surfaces deeper than 3 m depth existed in the dangerous zone. Slope failure would occur along 5 m depth slip surface as FS became critical value,

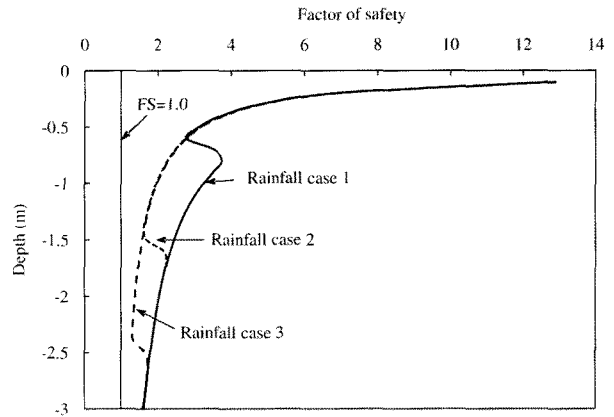


Fig. 17. Variations of FS along shallow slip surface for rainfall cases

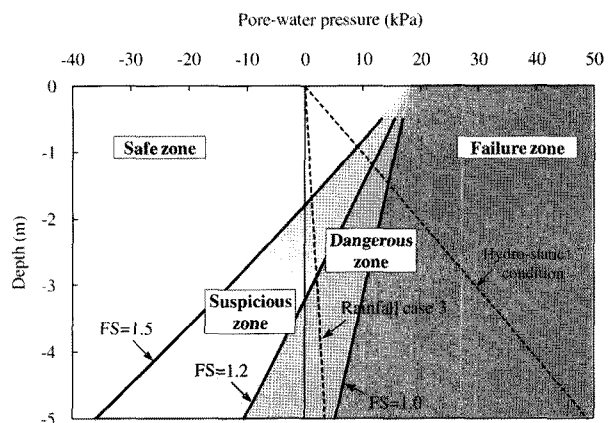


Fig. 18. Failure warning criteria of shallow slip surface

1.0. The critical depth of this slope could be defined as 3 m depth for the rainfall case 3. The slope would be also unstable if the measured pore-water pressure in 3 m depth is higher than 1.3 kPa.

There developed no positive pore-water pressures in the measurement results. According to the failure warning criteria, the monitored slope at shallow depth had sufficient stability for the rainfall infiltration. However, the simulated results showed that the slope failure could occur at deeper surface than the monitored depth. In this condition, measurement of matric suction or water content must be conducted up to at least 3 m depth.

## 7.2 Probabilistic Analysis

The reliability index of slope considering the measured matric suction was evaluated. Effective cohesion ( $c'$ ), friction angle ( $\phi'$ ), and matric suction ( $u_a - u_w$ ) were considered

Table 6. Input values of parameters used in probabilistic analysis

Input parameter	Mean value	C.O.V. (%)	Reference
Cohesion ( $c'$ )	10 kPa	40	Fredlund & Dahman (1971)
Friction angle ( $\phi'$ )	30	10	Phoon & Kulhawy (1999)
Matric suction ( $u_a - u_w$ )	0~70 kPa	20~50	Lee et al. (2008)
Unit weight ( $\gamma$ )	17.56 kN/m <sup>3</sup>		
Slope angle ( $\alpha$ )	30		
Depth ( $z$ )	0.15~0.6 m		

as random variables and assumed that the values have normal distribution. The input values of parameters used in this analysis are summarized in Table 6.

Limit state function can be defined as  $G(X)=FS(X)-1$  for general stability problems. For rainfall-induced slope stability problem with random variables such as cohesion  $c'$ , friction angle  $\phi'$ , matric suction ( $u_a - u_w$ ) and factor of safety which were expressed by Eq. (11), the limit state surface can be expressed as

$$G(c', \phi', (u_a - u_w)) = \frac{c' + \{\gamma z_w \cos^2 \alpha + (u_a - u_w)\} \tan \phi'}{\gamma z \sin \alpha \cos \alpha} - 1 \quad (13)$$

The reliability index was calculated by AFORM (Advanced First Order Reliability Method) (Hasofer & Lind, 1974) as follows.

$$\beta_{HL} = \min_{Z \in F} \sqrt{Z^T R^{-1} Z} \quad (14)$$

$$Z = \frac{x - \mu}{\sigma} \quad (15)$$

where,  $Z$  = vector of standard normalized random variables;  $x$  = vector of random variables;  $\mu$  = vector of mean value;  $\sigma$  = standard deviation of random variables;  $R$  = correlation matrix; and  $F$  = failure region.

Fig. 19 plots variations of matric suction, reliability index and FS calculated from the data monitored in the field in 2-D visualization according to date. During rainstorm, all depths have low value of matric suction, and the factor of safety and the reliability index decreased. After rainfall, the stability of slope recovered from the surface in order.

The matric suction variation is the most significant factor to affect the reliability index and the change of matric suction at surface is larger than that at deeper depth.

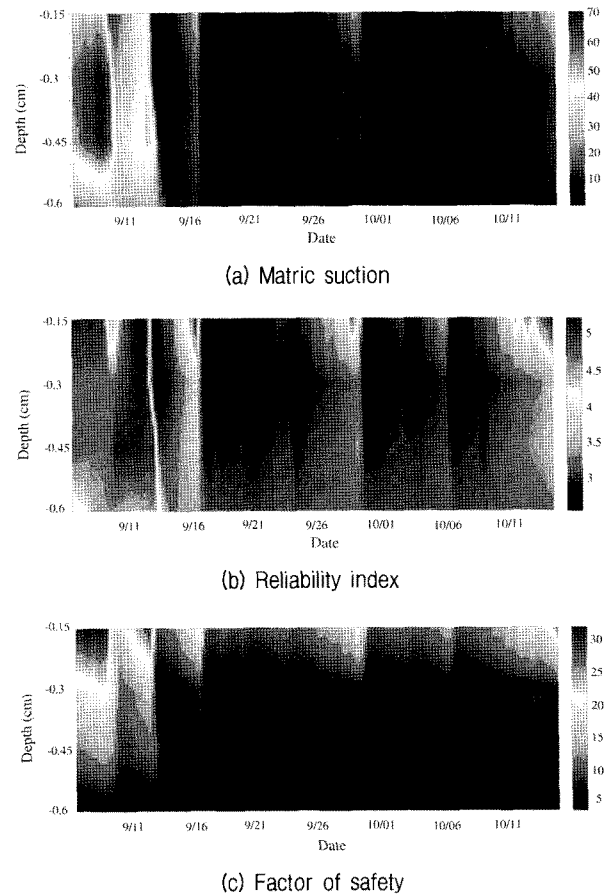


Fig. 19. 2D visualization of slope stability results

According to the results, control of rainfall infiltration into slope would be the most effective way of increasing the stability. The above analysis results indicate that the probability of failure at every depth with time can be effectively quantified by the suggested method.

## 8. Conclusions

It is necessary to consider the effect of rainfall infiltration into slope in the stage of slope design to prevent sudden failures of slopes due to rainfall. A slope design method

was suggested to evaluate the slope instability considering the rainfall infiltration. For a numerical analysis, unsaturated soil properties such as soil-water characteristic curve and unsaturated permeability function were simply estimated.

Soil properties measured in a real field slope were monitored in real-time and used to evaluate failure warning criteria based on deterministic and probabilistic analyses. The application validates that the reliability based slope assessment method considering the measured matric suction variation is capable of quantifying the slope risk and hence it can be an effective technique for slope monitoring and maintenance.

### Acknowledgements

The research reported in this paper was supported by Smart Infra-Structure Technology Center (Engineering Research Center) under the sponsorship of KOSEF (Korea Science and Engineering Foundation).

### References

1. Arya, L. M., and Paris, J. F. (1981), "A physico-empirical model to predict the soil moisture characteristic from particle size distribution and bulk density data", *Soil Science American Journal*, Vol.45, pp.1023-1030.
2. Burdine, N. T. (1953), "Relative permeability calculations from pore size distribution data", *Journal of Petroleum Technology*, Vol.5, No.3, pp.71-78.
3. Cho, S.E., and Lee, S.R. (2002), "Evaluation of surficial stability for homogeneous slopes considering rainfall characteristics", *Journal of Geotechnical and Geoenvironmental Engineering*, ASCE, Vol.128, No.9, pp.756-763.
4. Cui, J. (2007), Prediction of permeability for unsaturated weathered granite soils based on soil-water characteristic curve, Master's thesis, KAIST (In Korean).
5. Escario, V., and Juca, J. (1989), "Strength and deformation of partly saturated soils", *Proceedings of the 12th International Conference on soil Mechanics and Foundation Engineering*, Rio de Janeiro, Vol.3, pp.43-46.
6. Fourie, A.B., Rowe, D., and Blight, G.E. (1999), "The effect of infiltration on the stability of the slopes of a dry ash dump", *Geotechnique*, Vol.49, No.1, pp.1-13.
7. Fredlund, D. G. (1995), "The stability of slopes with negative pore-water pressure", *Proceedings, Ian Boyd Donald Symposium on Modern Developments in Geomechanics*, Monash University, Melbourne, Australia, June 7, pp.99-116.
8. Fredlund, D. G., Morgenstern, N. R., and Widger, R. A. (1978), "Shear strength of unsaturated soils", *Canadian Geotechnical Journal*, Vol.15, No.3, pp.313-321.
9. Gan, J. K. M., and Fredlund, D. G., and Rahardjo, H. (1988), "Determination of the shear strength parameters of an unsaturated soil using the direct shear test", *Canadian Geotechnical Journal*, Vol.25, pp.500-510.
10. Hasofer, A. M., and Lind, N. C. (1974), "Exact and Invariant Second-moment Code Format", *Journal of Engineering Mechanics Division*, ASCE, Vol.100, No.1, pp.111-121.
11. Kim, Y. K. (2003), Permeability of unsaturated weathered soils by analyzing triaxial permeameter test results, Master's thesis, KAIST (In Korean).
12. Lee, S. J. (2004), Estimation of unsaturated shear strength and soil water characteristic curve for weathered granite soil, Doctoral thesis, KAIST.
13. Lee, S. J., Lee, S. R., and Kim, Y. S. (2003), "An approach to estimate unsaturated shear strength using artificial neural network and hyperbolic formulation", *Computers and Geotechnics*, Vol.30, pp.489-503.
14. Lee, S. R., Choi, J. C., Kim, Y. K. (2008), "Reliability Based Real-time Slope Stability Assessment", *Proceedings of KGS Fall National Conference 2008*, Gwangju, Korea, pp.427-435.
15. Mualem, Y. (1976), "A new model for prediction the hydraulic conductivity of unsaturated porous media", *Water Resources Research*, Vol.12, pp.513-522.
16. Rahardjo, H., Lim, T.T., Chang, M.F., and Fredlund, D.G. (1994), "Shear-strength characteristics of a residual soil", *Canadian Geotechnical Journal*, Vol.32, pp.60-77.
17. Rawls, W. J., and Brakensiek, D. L. (1985), "Prediction of soil water properties for hydrologic modeling", In E. B. Jones and T. J. Ward(Eds). *Watershed Management in the Eighties. Proc. Of Symp. Sponsored by Comm. On Watershed Management*, I & D Division, ASCE Convention, Denver, Co, April 30-May 1, pp.293-299.

(접수일자 2009. 3. 9, 심사완료일 2009. 5. 28)